

MINISTRY OF EDUCATION
AND TRAINING

VIETNAM ACADEMY OF
SCIENCE AND TECHNOLOGY

GRADUATE UNIVERSITY SCIENCE AND TECHNOLOGY



NGUYEN MINH TRIEU

**RESEARCH AND DEVELOPMENT OF CHATTERING FREE
SLIDING MODE CONTROL METHOD FOR ELECTRICAL
SERVO DRIVES**

**SUMMARY OF DISSERTATION ON ELECTRICAL,
ELECTRONICS, AND TELECOMMUNICATION**

Major: Control Engineering and Automation

Code: 9 52 02 16

Ha Noi – 2026

The dissertation is completed at: Graduate University of Science and Technology, Vietnam Academy Science and Technology

Supervisors:

1. **Supervisors 1:** Prof. Dr. Nguyen Truong Thinh, College of Technology and Design, University of Economics Ho Chi Minh City
2. **Supervisors 2:** Dr. Tran Trong Toan, Institute of Information Technology, Vietnam Academy of Science and Technology, Ho Chi Minh City, Viet Nam

Referee 1: Assoc. Prof. Dr. Phan Cong Binh, Ho Chi Minh City University of Technology and Engineering

Referee 2: Dr. Nguyen Nhu Son, Institute of Information Technology, Vietnam Academy of Science and Technology

The dissertation is examined by Examination Board of Graduate University of Science and Technology, Vietnam Academy of Science and Technology at 8:30 AM, May 9, 2026.

The dissertation can be found at:

1. Graduate University of Science and Technology Library
2. National Library of Vietnam

INRODUCTION

1. The necessity of a dissertation

Sliding Mode Control (SMC) has been proposed as a robust control method [1]. In practice, the implementation of classical sliding mode controllers encounters two major problems, including chattering and the appearance of singularities in the control signal. Within the scope of this thesis, the electric motor is not the main focus, but is only used as a typical object to verify and evaluate the effectiveness of the proposed control method. The thesis focuses on developing a high-order TSM sliding mode control algorithm, including constructing the sliding surface, analyzing stability, designing the control law, and proving the convergence of the system.

For the above reasons, the dissertation focuses on minimizing robust chattering under model uncertainties and ensuring the system converges within a finite time. A new sliding surface is proposed by adding both the integral error and the state derivative to the NTSM sliding surface. Compared with the conventional NTSM controller, this sliding surface can handle higher-order derivatives. Therefore, the system error converges to zero within a finite time, with significantly reduced chattering.

2. Research objective

This study develops a PID-NTSM sliding mode controller with a layered structure, aiming to reduce chattering and avoid singularities in the control signal. The performance of the proposed controller is evaluated on an electric motor to improve the efficiency, reliability, and stability of electric motor systems in industrial and civil applications.

3. The main research contents

- Develop a high-order sliding mode controller with a cascaded structure to reduce chattering and avoid singularities.

- Apply the proposed controller to a DC motor.
- Apply the proposed controller to an IM motor.
- Demonstrated using Lyapunov stability theory and verified through simulations and experiments on the testbench.

The thesis structure consists of 4 chapters:

Chapter 1: Presents an overview of sliding mode control and its applications in motor control.

Chapter 2: The development of a higher-order SMC method called PID-NTSM.

Chapter 3: Application to DC motors.

Chapter 4: Application to three-phase asynchronous motors.

The final section of the dissertation presents the conclusions and future development directions.

Chapter 1. OVERVIEW

1.1. Introduction

Based on the gaps in research on sliding mode control, this thesis focuses on proposing a new sliding surface design to address the following key issues:

- i. Minimizing chattering while maintaining the robustness of the SMC;
- ii. Ensure convergence in a finite time and improve the convergence time;
- iii. Avoiding singularities in the control signal.

1.2. Literature review

Sliding Mode Control (SMC) is a very popular control method due to its simplicity and ability to resist uncertainty and disturbances. A stable and robust platform is built on the principles of Lyapunov theory. Many control methods have been developed, such as Terminal Sliding Mode (TSM), Nonsingular TSM (NTSM), and Higher-Order SMC (HOSM) [2-4]. Or

algorithms such as super-twisting, high-order sliding manifolds HOTSM [5, 6], or combined with AI models have been implemented [7, 8].

Electric motors are the application of control algorithms [9, 10]. Many studies have been conducted to investigate the characteristics of DC electric motors [11-15]. Notable studies on asynchronous motors, such as [16-20], are based on the FOC control method. In addition, DTC has also been studied and developed; the main disadvantage of DTC is that it causes torque ripple and is difficult to control at low speeds [21-24].

Linear controllers such as PI and PID often experience performance degradation when model uncertainties are large [8, 25, 26]. Variations of controllers for electric motors have been studied, showing the strong capabilities of SMC against model disturbances and uncertainties [27-29]. Studies applying SMC to DC motors and asynchronous motors (IM) such as [30-33]. Studies on TSM for IM have been proposed by many studies [16], NTSM [34]; however, the chattering problem still exists.

This dissertation focuses on proposing a PID-NTSM controller to address the issues of chattering, convergence time, and robustness of sliding mode control, which is also the main contribution of the dissertation.

1.3. Methods in sliding mode control

1.3.1. Conventional linear sliding mode control

Consider a quadratic system with the following equations

$$\begin{cases} \dot{x}_1 = x_2 \\ \dot{x}_2 = -0.38x_2 + u - \sin(t) \end{cases} \quad (1.1)$$

where x_1, x_2 are state variables, u is the control signal, $\sin(t)$ is the external noise and is bounded by $\|\sin(t)\| \leq 1$. The parameters are set as follows $x_1(0)=4$, $x_2(0)=1$. The sliding surface is defined by the equation (1.2). The control signal $u(t)$ is designed as (1.3).

$$s = x_2 + \dot{x}_1 \quad (1.2)$$

$$u(t) = 0.38x_2 - \dot{x}_1 - 5\text{sign}(s) \quad (1.3)$$

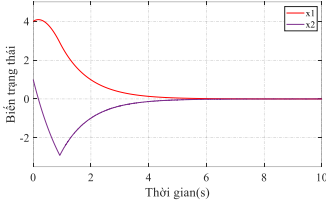


Figure 1.1. Response

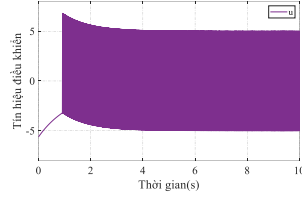


Figure 1.2. Control signal

1.3.2. High-Order Linear Sliding Mode Control

Consider a quadratic system similar to example 2.1 with the following initial parameters chosen as follows $x_1(0)=4$, $x_2(0)=1$. The sliding surface is chosen

$$s = \ddot{x}_1 + 3\dot{x}_1 + 2x_1 \quad (1.4)$$

The control law is designed as follows:

$$\begin{cases} u_{eq} = 0.38x_2 - 3\dot{x}_1 - 2x_1 \\ \dot{u}_n = -5\text{sign}(s) \end{cases} \quad (1.5)$$

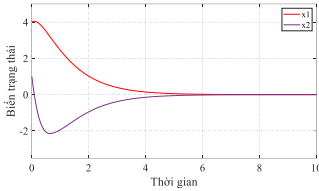


Figure 1. 3. Response

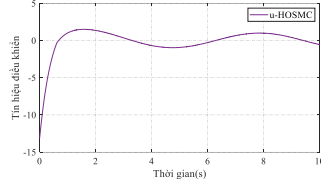


Figure 1.4. Control signal

1.3.3. Terminal Sliding Mode Control (TSM)

Consider a second-order system similar to example 2.1 with the following initial parameters chosen as follows: $x_1(0)=4$, $x_2(0)=1$. The sliding surface is defined as follows

$$s = x_2 + x_1^{3/5} \quad (1.6)$$

The control signal is designed as

$$u = 0.38x_2 - \frac{3}{5} \frac{1}{x_1^{2/5}} x_2 - 5\text{sign}(s) \quad (1.7)$$

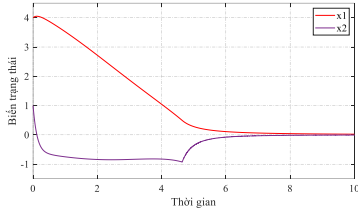


Figure 1. 5. Response

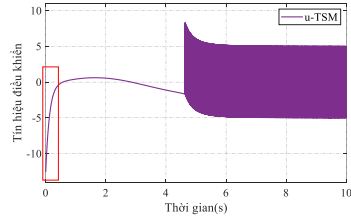


Figure 1. 6. Control signal

1.3.4. Nonsingular Terminal Sliding Mode Control (NTSM)

Consider a second-order system similar to example 1.1 with the following initial parameters chosen as follows $x_1(0)=4$, $x_2(0)=1$. The sliding surface is defined as follows

$$s = x_1 + x_2^{5/3} \quad (1.8)$$

The control signal is designed as

$$u(t) = 0.38x_2 - \frac{3}{5}x_2^{\left(2-\frac{5}{3}\right)} - 5\text{sign}(s) \quad (1.9)$$

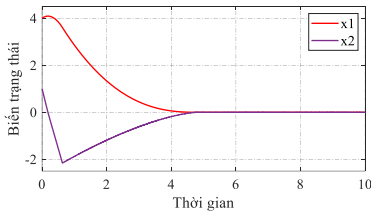


Figure 1. 7. Response

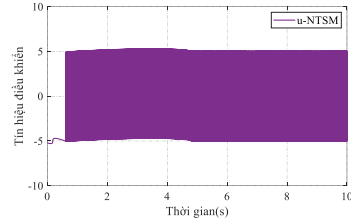


Figure 1. 8. Control signal

1.4. Chattering in sliding mode control

Chattering is a finite frequency and amplitude oscillation that often occurs in practical sliding mode controllers. It damages electromechanical devices due to intermittent operation or causes wear on actuators [35]. Reducing chattering is one of the important issues in the development of sliding mode control theory. Many studies strive to minimize the chattering of sliding mode controllers in order to bring them into practical applications [36, 37]. Studies aimed at reducing chattering and reducing the response time of the system are divided into three main types.

The first approach is to replace the sign function with saturation or sigmoid functions [38].

The second approach is to use a combination of different control methods to exploit the advantages of controllers such as neural networks, fuzzy control, and adaptive control [39-41].

The third approach is to propose new sliding mode control theories to maintain robust characteristics and aim to reduce chattering.

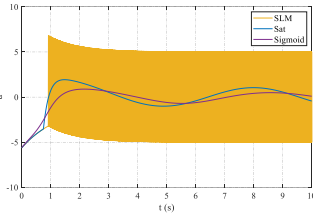


Figure 1. 9. Compare the control signals with the sigmoid and sat functions.

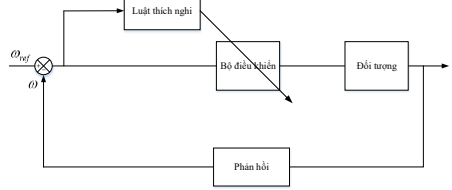


Figure 1. 10. A typical adaptive control model

1.5. Research issues in the dissertation

This dissertation proposes the development of a high-order NTSM sliding mode control based on a hierarchical structure aimed at achieving convergence in finite time with nonsingular, particularly significantly reducing chattering without compromising system stability. Various electric motor types are used for the performance evaluation of the proposed control method. Through this, the robustness of the method is confirmed for practical applications, addressing classic sliding mode control problems regarding chattering, convergence time, and stability.

Chapter 2. DEVELOPMENT OF HIGHER-ORDER SLIDING MODE CONTROL PID – NTSM

2.1. Sliding mode control theory

Consider nonlinear systems such as (2.1).

$$x = f(x), f(0) = 0, x \in R^n \quad (2.1)$$

Definition 2.1 [1]. The equilibrium point $x = 0$ is called asymptotically stable if it satisfies

1. Stabilization according to Lyapunov, i.e.

$$\forall \varepsilon > 0, \exists \delta > 0 : \|x(0)\| < \delta \Rightarrow \|x(t)\| < \varepsilon, \forall t \geq 0.$$

2. Convergence to the zero, i.e.

$$\lim_{t \rightarrow \infty} x(t) = 0$$

Theorem 2.1 [1]. Let $x = 0$ be the asymptotically stable point of the system (2.1), $D \subset R^n$ is the region containing that equilibrium point, assume there exists a continuously differentiable Lyapunov function satisfying the following conditions:

$$\begin{cases} V > 0, \forall x \neq 0, V(0) = 0 \\ \dot{V} < 0 \end{cases} \quad (2.2)$$

Then, the equilibrium point $x = 0$ is stable according to Lyapunov.

The condition exists (2.3).

$$\dot{V} = \nabla V^T f(x) \leq -\alpha V(x), \quad \forall x \neq 0 \quad (2.3)$$

where $\alpha > 0$ is a constant.

In that case, the origin $x = 0$ is the asymptotically stable point, and the solution converges according to an exponential function (2.4).

$$V(x(t)) \leq V(x(0))e^{-\alpha t}, \quad \forall t \geq 0 \quad (2.4)$$

Definition 2.2 [2]. An equilibrium point $x = 0$ is called asymptotically stable in finite time if there exists a finite time point $T < \infty$ such that

1. Stabilization according to Lyapunov, i.e.

$$\forall \varepsilon > 0, \exists \delta > 0 : \|x(0)\| < \delta \Rightarrow \|x(t)\| < \varepsilon, \forall t \in [0, T]$$

2. Convergence in a finite time, i.e.

$$\exists T < \infty : x(t) = 0, \forall t \geq T \quad \square$$

Theorem 2.2. [2] Let $x = 0$ be the equilibrium point of the system (2.1), $D \subset R^n$ is the region containing that equilibrium point, assuming a Lyapunov

function exists $V : D \rightarrow R$ that is continuously differentiable and satisfies the following conditions.

$$\dot{V}(x) \leq -cV^\beta(x), \quad \forall x \neq 0 \quad (2.5)$$

where, $c > 0$ and $0 < \beta < 1$.

Then, the origin $x=0$ is a stable point in finite time. Specifically, for every solution starting from $x(0)$, the function $V(T) = 0$ in time T does not exceed.

$$T \leq \frac{V^{1-\beta}(0)}{c(1-\beta)} \quad (2.6)$$

2.2. Evaluation of Chattering in Sliding Mode Control

Analytical metrics such as ISE and IAE can be extended to evaluate chattering by applying them to the control signal or sliding mode variable, calculated using a formula (2.7)(2.8) .

$$ISE = \int u^2(t)dt \quad (2.7)$$

$$IAE = \int |u(t)|dt \quad (2.8)$$

2.3. Design of a higher-order PID nested NTSM controller

2.3.1. First-order nonlinear system

Consider a first-order nonlinear system such as (2.9).

$$\dot{x} = f(x, t) + g_n u + d(x, t) \quad (2.9)$$

Assumption 2.1. The second derivative of $d(t)$ is bounded by

$$|\ddot{d}(x, t)| \leq \phi \quad (2.10)$$

The sliding surface l is proposed as equation (3.3) with s defined as (3.4).

This is a significant contribution of the thesis.

$$l = s + \gamma \dot{s}^{p/q} \quad (2.11)$$

$$s = \zeta_1 x(t) + \zeta_2 \int_0^t x(t)dt + \zeta_3 \frac{dx}{dt} \quad (2.12)$$

Theorem 2.1. Consider the nonlinear system as (2.9), if the sliding surface l is chosen according to (2.11), with the sliding variable s as (2.12), and the control signal is designed according to equations

$$u = u_{eq} + u_n \quad (2.13)$$

$$u_{eq} = \frac{1}{g_n \zeta_3} \int_0^t (-\zeta_1 \dot{x}_1 - \zeta_2 x_1 - \zeta_3 \dot{f}(x)) dt \quad (2.14)$$

$$u_n = \frac{1}{g_n \zeta_3} \int_0^t \int_0^s [-K \text{sign}(l) - \mu l - \frac{q}{p} \gamma^{-1} \dot{s}^{(2-p/q)}] dt_1 dt \quad (2.15)$$

Then the system's trajectory moves towards the sliding surface in a finite time, and the system's state converges asymptotically to zero. \square

Proof of Theorem 2.1. Choose the Lyapunov function $V=0.5l^2$

Consider the time derivative of the Lyapunov function V and ensure that $\dot{V} < 0$, the time derivative of V can be rewritten as an equation (2.16).

$$\begin{aligned} \dot{V} &= \dot{l} \\ &= l \left[\gamma \frac{p}{q} \dot{s}^{(p/q-1)} \left(\ddot{s} + \gamma^{-1} \frac{q}{p} \dot{s}^{(2-p/q)} \right) \right] \\ &= -\frac{p}{q} l \gamma \dot{s}^{(p/q-1)} (K \text{sign}(l) + \mu l - \zeta_3 \ddot{d}(t)) \\ &= -\frac{p}{q} \gamma \dot{s}^{(p/q-1)} (K|l| + \mu l^2 - \zeta_3 l \ddot{d}(t)) \end{aligned} \quad (2.16)$$

The coefficient K is chosen according to assumption 2.1. In this case, $\dot{s}^{(p/q-1)} > 0$, then \dot{V} becomes

$$\dot{V} \leq -\gamma \frac{p}{q} \dot{s}^{(p/q-1)} \eta |l| < 0, \quad \forall l \neq 0 \quad (2.17)$$

where, $K - \zeta_3 \phi = \eta > 0$.

2.2.2. Second-order nonlinear system

Consider a second-order nonlinear system defined as (2.18).

$$\begin{cases} \dot{x}_1 = x_2 \\ \dot{x}_2 = f(x) + g_n u + d(t) \end{cases} \quad (2.18)$$

Assumption 2.2. The derivative of $d(t)$ is bounded by

$$\left| \dot{d}(x, t) \right| \leq \phi \quad (2.19)$$

The sliding surface l is proposed as equation (2.12) with s defined as (2.21).

$$l = s + \gamma \dot{s}^{p/q} \quad (2.20)$$

$$s = \zeta_1 x_1 + \zeta_2 \int_0^t x_1 dt + \zeta_3 x_2 \quad (2.21)$$

Theorem 2.2. *Consider the second-order nonlinear system described by (2.10). If the sliding surface l is chosen according to (2.12), with the sliding variable s defined by (2.13), and the control signal is designed as*

$$u = u_{eq} + u_n \quad (2.22)$$

$$u_{eq} = \frac{1}{g_n \zeta_3} (-\zeta_1 x_2 - \zeta_2 x_1 - \zeta_3 f(x)) \quad (2.23)$$

$$u_n = \frac{1}{g_n \zeta_3} \int_0^t \left(-K \text{sign}(l) - \mu l - \frac{q}{p} \gamma^{-1} \dot{s}^{(2-p/q)} \right) dt \quad (2.24)$$

Then the system's trajectory moves towards the sliding surface in a finite time, and the system's state variables converge asymptotically to 0. \square

Proof of Theorem 2.2. Choose the Lyapunov function $V=0.5l^2$

Consider the time derivative of the Lyapunov function V and ensure that $\dot{V} < 0$, the time derivative of V can be rewritten as an equation (2.25).

$$\begin{aligned} \dot{V} &= l \dot{l} \\ &= l \left[\gamma \frac{p}{q} \dot{s}^{(p/q-1)} \left(\ddot{s} + \gamma^{-1} \frac{q}{p} \dot{s}^{(2-p/q)} \right) \right] \\ &= l \left[\gamma \frac{p}{q} \dot{s}^{(p/q-1)} \left(-K \text{sign}(l) - \mu l + \zeta_3 \dot{d}(t) \right) \right] \\ &= -\gamma \frac{p}{q} \dot{s}^{(p/q-1)} \left(K |l| + \mu l^2 - \zeta_3 l \dot{d}(t) \right) \end{aligned} \quad (2.25)$$

The coefficient K is chosen according to assumption 2.2. In this case, $\dot{s}^{(p/q-1)} > 0$, then \dot{V} becomes

$$\dot{V} \leq -\gamma \frac{p}{q} \dot{s}^{\left(\frac{p}{q}-1\right)} \eta |l| < 0, \quad \forall l \neq 0 \quad (2.26)$$

where, $K - \zeta_3 \phi = \eta > 0$.

2.4. Simulation

Consider the first-order system as (2.27).

$$\dot{x}_1 = -0.38x_1 + u + 0.1 \sin(t) \quad (2.27)$$

Controller $u = u_n + u_{eq}$ is designed as (2.28) based on Theorem 2.1.

$$\begin{cases} u_{eq} = \frac{1}{\zeta_3} \int_0^t (-\zeta_1 - 0.38\zeta_3) \dot{x}_1 - \zeta_2 x_1 dt \\ u_n = \frac{1}{\zeta_3} \int_0^t \int_0^t \left[-K \text{sign}(l) - \mu l - \frac{q}{p} \gamma^{-1} \dot{s}^{\left(\frac{2-p}{q}\right)} \right] dt_1 dt \end{cases} \quad (2.28)$$

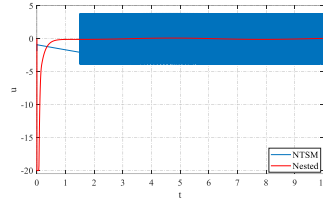
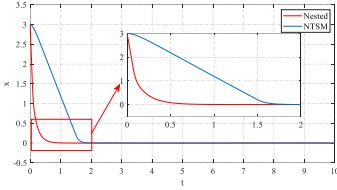


Figure 2.1. Response

Figure 2.2. Control signal

Table 2.1. ISE và IAE đánh giá chattering trong tín hiệu điều khiển

	ISE	IAE	Decrease ISE (%)	Decrease IAE (%)
NTSM	120.033	31.802	-	-
PID - NSTM	0.040	0.523	99.97	98.35

Consider a second-order nonlinear system (2.29)

$$\begin{cases} \dot{x}_1 = x_2 \\ \dot{x}_2 = -0.38x_2 + u + 0.1 \sin(t) \end{cases} \quad (2.29)$$

Based on Theorem 2.2, the control law $u = u_{eq} + u_n$ is designed as (2.30)

$$\begin{cases} u_{eq} = \frac{1}{\zeta_3} ((-\zeta_1 x_2 - \zeta_2 x_1 - \zeta_3 0.38 x_2)) \\ u_n = \frac{1}{\zeta_3} \int_0^t \left(-K \text{sign}(l) - \mu l - \frac{q}{p} \gamma^{-1} \dot{s}^{\left(\frac{2-p}{q}\right)} \right) dt \end{cases} \quad (2.30)$$

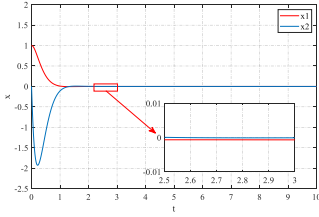


Figure 2.3. Response

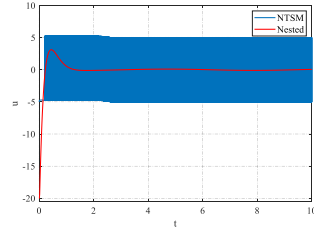


Figure 2.4. Control signal.

Table 2.2. ISE and IAE to evaluate chattering

	ISE	IAE	Decrease ISE (%)	Decrease IAE (%)
NTSM	226.324	45.122	-	-
PID - NSTM	0.068	0.612	99.97	98.64

Chapter 3. APPLICATIONS ON DC MOTORS

3.1. Introduction to electric motor systems and modeling

DC electric motors are used in many applications such as robotics, automation, and industrial systems with high requirements for accuracy, fast response, and high efficiency [42-44]. The dynamic model of an ideal motor is calculated based on Kirchhoff's and Newton's laws as (3.1).

$$\begin{cases} \hat{L}\dot{i} = -\hat{R}i - E + u + d(t) \\ \hat{J}\dot{\omega} = K_m i - T_L - \hat{b}\omega + \rho(t) \end{cases} \quad (3.1)$$

Converting it to the standard equation form in Chapter 3, the system error equation is defined as follows (4.2).

$$\dot{\hat{x}}(t) = \underbrace{-\alpha_2 \hat{e}_\omega(t)}_{f(x)} - \underbrace{\alpha_1 i(t)}_{g_n} + d(t) \quad (3.2)$$

where $\alpha_1 = \frac{K_m}{J}$; $\alpha_2 = \frac{\hat{b}}{J}$; $d(t) = \frac{1}{J}\dot{T}_L(t) - \frac{1}{J}\dot{\rho}(t) + \ddot{\omega}_{ref} + \alpha_2\dot{\omega}_{ref}$ is the total uncertainty and disturbances.

3.2. Conventional sliding mode controllers

Assumption 3.1. $d(t)$ is bounded by ϕ .

$$|d(t)| \leq \phi \quad (3.3)$$

3.2.1 Linear sliding mode controller

The sliding surface of the SLM is designed as (3.4).

$$s = \gamma e_\omega \quad (3.4)$$

The control law is designed as (3.5) - (3.7).

$$i = i_{eq} + i_n \quad (3.5)$$

$$i_{eq} = \frac{1}{\alpha_1} (\dot{\omega}_{ref} - \alpha_2 \omega_{ref} + \alpha_2 e_\omega) \quad (3.6)$$

$$i_n = \frac{1}{\gamma \alpha_1} (K \text{sign}(s) + \mu s) \quad (3.7)$$

3.2.2 NTSM controller

The NTSM sliding surface is applied as (3.8).

$$s = e_\omega + \gamma \dot{e}_\omega^{p/q} \quad (3.8)$$

The control law is designed as (3.9) - (3.11).

$$i = i_{eq} + i_n \quad (3.9)$$

$$i_{eq} = \frac{1}{\alpha_1} \alpha_2 e_\omega \quad (3.10)$$

$$i_n = \frac{1}{\alpha_1} \int_0^t \left(K \text{sign}(s) + \mu s + \frac{q}{p} \gamma^{-1} \dot{e}_\omega^{(2-p/q)} \right) dt \quad (3.11)$$

3.3. PID - NTSM controller

The higher-order NSTM sliding surface l is introduced by equation (3.12), with s defined in equation (3.13).

$$l = s + \gamma \dot{s}^{p/q} \quad (3.12)$$

$$s = \zeta_1 e_\omega + \zeta_2 \int_0^t e_\omega dt + \zeta_3 \frac{de_\omega}{dt} \quad (3.13)$$

Assumption 3.2. $d(t)$ is bounded by the coefficient ϕ as in formula (3.15).

$$|\ddot{d}(t)| \leq \phi \quad (3.14)$$

where $\phi > 0$.

Theorem 3.1. Consider the motor error dynamics described by (4.2), if the slip surface is selected according to (4.12) - (4.13) and the control signal is designed according to (4.15) - (4.17).

$$i = i_{eq} + i_n \quad (3.15)$$

$$i_{eq} = \frac{1}{\mu_3} \int_0^t (\zeta_3 \dot{\omega} + \mu_1 \dot{e}_\omega + \mu_2 e_\omega) dt \quad (3.16)$$

$$i_n = \frac{1}{\mu_3} \int_0^t \int_0^{t_1} \left(K \text{sign}(l) + \mu l + \frac{q}{p} \gamma^{-1} \dot{s}^{(2-p/q)} \right) dt_1 dt \quad (3.17)$$

where K is the control coefficient, positive; μ is the adjustment coefficient, positive; $\mu_1 = \zeta_1 - \zeta_3 \alpha_2$, $\mu_2 = \zeta_2$ $\forall \alpha$ $\mu_3 = \zeta_2 \alpha_1$.

The error trajectory of the system advances towards the sliding surface in a finite time and converges according to Lyapunov stability theory. \square

Proof of Theorem 3.1. Choose the Lyapunov function $V=0.5l^2$

The time derivative of V can be rewritten as an equation

$$\begin{aligned} \dot{V} &= l\dot{l} \\ &= l \left[\gamma \frac{p}{q} \dot{s}^{(p/q-1)} \left(\dot{s} + \gamma^{-1} \frac{q}{p} \dot{s}^{(2-p/q)} \right) \right] \\ &= l \left[\gamma \frac{p}{q} \dot{s}^{(p/q-1)} \left(-K \text{sign}(l) - \mu l + \zeta_3 \ddot{\omega}(t) \right) \right] \\ &= -\gamma \frac{p}{q} \dot{s}^{(p/q-1)} \left(K |l| + \mu l^2 - \zeta_3 l \ddot{\omega}(t) \right) \end{aligned} \quad (3.18)$$

In the case, $\dot{s}^{(p/q-1)} > 0$ then \dot{V} can be considered as an equation

$$\dot{V} \leq -\gamma \frac{p}{q} \dot{s}^{(p/q-1)} \eta |l| < 0, \quad \forall l \neq 0 \quad (3.19)$$

where, $\eta = K - \zeta_3 \phi > 0$.

A PD controller is used in the inner loop to regulate the motor current.

The current control law is designed.

$$u = K_p e_i + K_d \dot{e}_i + K_e \omega \quad (3.20)$$

3.4. Simulation

Parameter	Symbol	Value
Resistance	R	1.6Ω
Inductance	L	0.0052 H
Back-emf voltage	K_e	0.011 V/rpm
Moment of inertia	J	0.0043 kg.m^2

The controller is designed based on Theorem 3.3 with the following computational and parameter selections: $p=5$, $q=3$, $\gamma=0,0001$, with $\zeta=1$ and $\omega_n=500$.

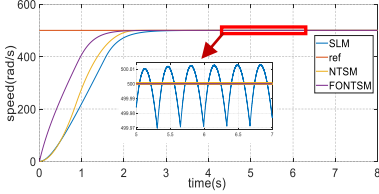


Figure 3. 1. Response

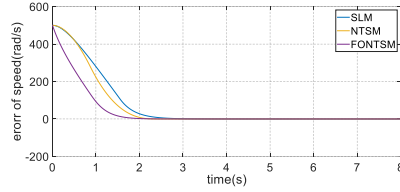


Figure 3. 2. Error

Table 3. 1. Comparison of ISE and IAE of SLM, NTSM, and PID-NTSM

	ISE $\times 10^{-5}$	IAE $\times 10^{-3}$
SLM	22.61	24.08
NTSM	14.28	8.97
PID-NTSM	0.81	0.07

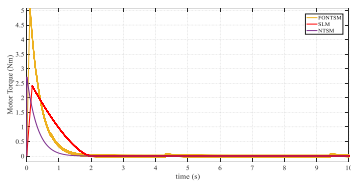


Figure 3. 3. Comparing the torque of different control methods

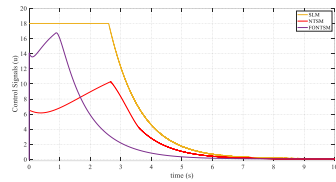


Figure 3. 4. Compare the control signals.

Let's assume the engine parameters are three times higher than the engine specifications.

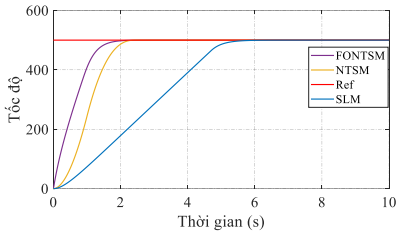


Figure 3.4. Controller response when parameters increase threefold

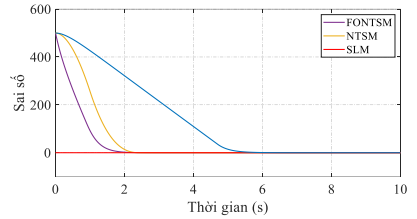


Figure 3.5. The controllers' errors

3.5. Experiment

To evaluate the practical applicability and performance of the proposed controller, a DC motor test bench was set up as follows.

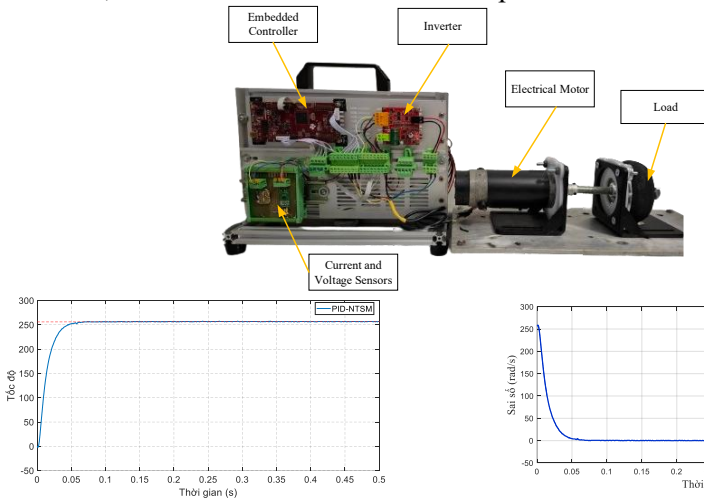


Figure 3.6. Response of the proposed controller.

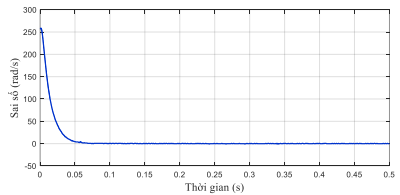


Figure 3.7. Actual proposed controller error

The content presents the application of the PID nested controller NTSM on DC motors, with the theoretical proposal in Chapter 2, and demonstrates its effectiveness. A paper is published based on the research content of Chapter 3 [CT.1].

Chapter 4. APPLICATIONS ON THREE-PHASE ASYNCHRONOUS MOTORS

4.1. Coordinate systems and modeling of three-phase asynchronous electric motors

Coordinate	Dimensions	Signal	Applications
abc	3	AC	Physical simulation, primary analysis
$\alpha\beta$	2	AC	PWM modulation, space vector representation
dq	2	DC	Torque-flux control

In this thesis, the dynamics of stator current, rotor flux, and rotor speed are expressed as equations in the d - q coordinate system. (4.1).

$$\begin{cases} \dot{i}_{sd} = \xi \frac{1}{T_r} \psi_r - \lambda i_{sd} + \omega_s i_{sq} + K u_{sd} \\ \dot{i}_{sq} = -\xi \omega \psi_r - \omega_s i_{sd} - \lambda i_{sq} + K u_{sq} \\ \dot{\psi}_r = -\frac{\hat{L}_m}{T_r^2 (\omega_s - \omega)} i_{sq} + \frac{\hat{L}_m}{T_r} i_{sd} \\ \dot{\omega}_m = \frac{n_p \hat{L}_m}{J \hat{L}_r} i_{sq} \psi_r - \frac{1}{J} (T_L + d(t)) \end{cases} \quad (4.1)$$

The motor speed error is defined as the deviation of the set speed from the actual motor speed as follows.

$$e_\omega = \omega_{mref} - \omega_m \quad (4.2)$$

Converting to the standard nonlinear system equation form, we have

$$\dot{x}(t) = \underbrace{\dot{\omega}_{ref}(t)}_{f(x)} - \alpha_1 \underbrace{i_{sq}(t)}_{z_n} + \alpha_2 \underbrace{\rho(t)}_{d(t)} \quad (4.3)$$

4.2. Conventional sliding mode controllers

Assumption 4.1. $\dot{\rho}(t)$ is bounded by ϕ .

$$|\dot{\rho}(t)| \leq \phi \quad (4.4)$$

4.2.1 Linear sliding mode controller

The sliding surface of the SLM is designed as

$$s = \gamma e_\omega \quad (4.5)$$

The control law is designed as

$$i_{sq} = i_{sqeq} + i_{sqn} \quad (4.6)$$

$$i_{sqeq} = \frac{1}{\gamma\alpha_1} \dot{\omega}_{ref} \quad (4.7)$$

$$i_{sqn} = \frac{1}{\gamma\alpha_1} (Ksign(s) + \mu s) \quad (4.8)$$

4.2.2. NTSM controller

The NTSM sliding surface is applied as.

$$s = e_\omega + \gamma \dot{e}_\omega^{p/q} \quad (4.9)$$

The control law is designed as

$$i_{sq} = i_{sqeq} + i_{sqn} \quad (4.10)$$

$$i_{sqeq} = \frac{1}{\alpha_1} \dot{\omega}_{ref} \quad (4.11)$$

$$i_{sqn} = \frac{1}{\alpha_1} \int \left(Ksign(s) + \mu s + \frac{q}{p} \gamma^{-1} \dot{e}_\omega^{(2-p/q)} \right) dt \quad (4.12)$$

4.3. PID - NTSM controller

The higher-order PID nested NTSM sliding surface is introduced by equation (4.13), with s defined in equation (4.14).

$$l_\omega = s_\omega + \gamma \dot{s}_\omega^{p/q} \quad (4.13)$$

$$s_\omega = \zeta_1 e_\omega(t) + \zeta_2 \int_0^t e_\omega(t) dt + \zeta_3 \frac{de_\omega}{dt} \quad (4.14)$$

Theorem 4.1. Consider the speed error dynamics of the motor in equation (5.3), if the sliding surface is selected according to (5.13–5.14) and the control law is designed as follows

$$i_{sq} = i_{sqeq} + i_{sqn} \quad (4.15)$$

$$i_{sqeq}(t) = \frac{1}{\zeta_3 \alpha_1} \int_0^t (\zeta_1 \dot{e}_\omega(t) + \zeta_2 e_\omega(t) + \zeta_3 \ddot{\omega}_{mref}(t)) dt \quad (4.16)$$

$$i_{sqn}(t) = \frac{1}{\zeta_3 \alpha_1} \int_0^t \int_0^t \left[K \text{sign}(l) + \mu l + \frac{q}{p} \gamma^{-1} \dot{s}^{(2-p/q)} \right] dt_1 dt \quad (4.17)$$

where K is the sliding coefficient, and μ is the adjustment coefficient.

In this case, the system's error trajectory is guaranteed to approach the sliding surface within a finite time. After reaching the sliding surface, the sliding motion is maintained, and the error converge asymptotically to zero.

Proof of Theorem 4.1. Choose the Lyapunov function $V=0.5l^2$

The time derivative of V can be rewritten as an equation

$$\begin{aligned} \dot{V} &= l \left[\gamma \frac{p}{q} \dot{s}^{(p/q-1)} \left(\ddot{s} + \gamma^{-1} \frac{q}{p} \dot{s}^{(2-p/q)} \right) \right] \\ &= \gamma l \frac{p}{q} \dot{s}^{(p/q-1)} [-K \text{sign}(l) - \mu l + \zeta_3 \alpha_2 \ddot{\rho}(t)] \\ &= -\gamma \frac{p}{q} \dot{s}^{(p/q-1)} (K |l| + \mu l^2 - \zeta_3 \alpha_2 l \ddot{\rho}(t)) \end{aligned} \quad (4.18)$$

The derivative equation of V can be rewritten as follows

$$\dot{V} \leq -\gamma \frac{p}{q} \dot{s}^{(p/q-1)} \eta |l| < 0, \quad \forall l \neq 0 \quad (4.19)$$

where, $\eta = K - \zeta_3 \alpha_2 \phi > 0$.

4.4. Simulation

Table 4. 1. Specifications of the Induction motor

Parameter	Symbol	Value
Rated power	P	180W
Rated voltage	V	36V
Rated frequency	f	50 Hz
Stator resistance	Rs	0.01485 Ω
Stator leakage inductance	Lls	0.3027 mH
Mutual inductance	Lm	0.01046 H
Rotor resistance	Rr	0.009295 Ω
Rotor leakage inductance	Llr	0.3027 mH

To evaluate the effectiveness of the control methods, a simulation environment was set up using MATLAB Simulink with a sampling time of 0.5 ms.

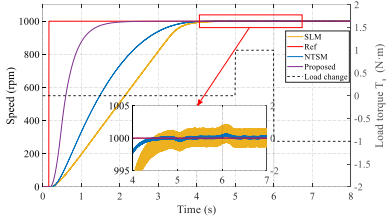


Figure 4.4. Speed response.

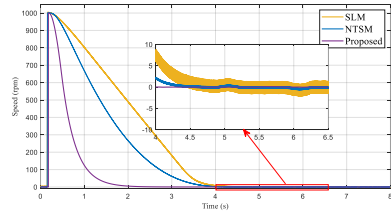


Figure 4.5. Speed error.

Table 4.2. Comparison of IAE and ISE controllers

Controller	IAE	ISE
Proposed	0.001	0.003
NTSM	0.438	0.822
SLM	1.933	2.272

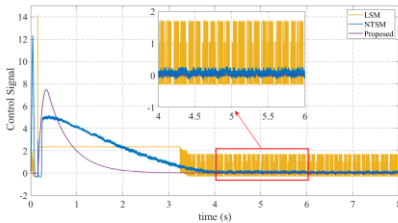


Figure 4.6. Control signal

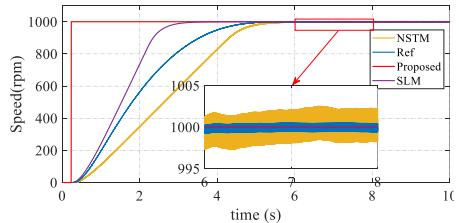


Figure 4.7. Response when the model parameter in the control law is 5 times the actual parameter

4.5. Experiment

The current on the q-axis approaches 0 after a short time, demonstrating the ability to reduce torque and control speed effectively, as shown in Figures 4.13–4.16.

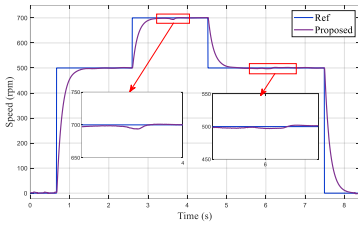
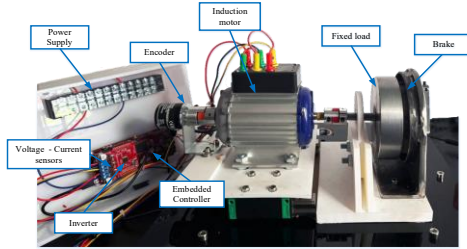


Figure 4.11. The actual motor speed response uses the proposed controller.

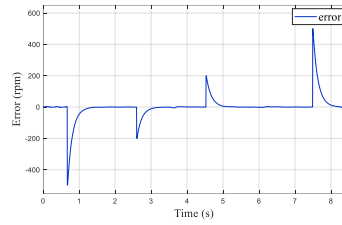


Figure 4.12. Actual error of the speed response for the proposed controller.

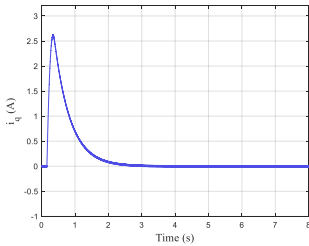


Figure 4.13. Current on the q-axis with $\omega_n = 500$ rpm

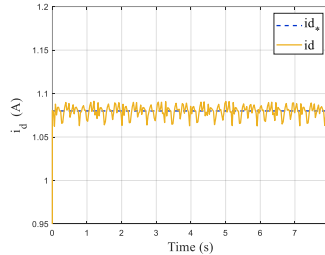


Figure 4.14. Current on the d-axis with $\omega_n = 500$ rpm

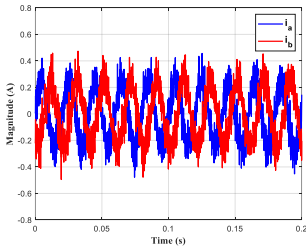


Figure 4.15. Current on the ab-axis with $\omega_n = 500$ rpm

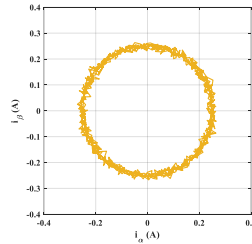


Figure 4.16. Phase of the current on the $\alpha\beta$ -axis

The content presents the complete design of SLM, NTSM, and nested NTSM PID controllers, demonstrating the effectiveness of the proposed controllers applied to a three-phase asynchronous motor with random load and model uncertainties. A research paper is published as part of the research in Chapter 4 [CT.2].

CONCLUSION AND FUTURE WORK

Main research contents of the dissertation

In this thesis, a sliding surface is proposed with the integration of the NTSM nonlinear sliding surface, where l is the principal sliding surface, and s is the PID sliding surface defined as follows.

$$l = s + \delta \dot{s}^{p/q}$$

$$s = \zeta_1 e(t) + \zeta_2 \int_0^t e(t) dt + \zeta_3 \dot{e}(t)$$

The main contributions of this dissertation include

- This dissertation proposes a new nested PID Nonsingular Terminal Sliding Mode (PID-NTSM) sliding surface structure for noisy and uncertain nonlinear systems. The proposed structure combines the advantages of both PID and NTSM sliding surfaces, maintaining the robustness characteristic of sliding mode control while significantly reducing chattering. Embedding the PID structure within the NTSM sliding surface elevates the sliding surface order, improves error dynamics, and smooths the control signal.

- Control laws are developed, and system stability is demonstrated based on Lyapunov theory, ensuring the existence and convergence of the sliding surface. Systematic analyses are conducted for both general nonlinear systems and electric drive systems, contributing to the development of layered higher-order sliding mode control research.

- The effectiveness of the method is verified on real-world electric drive systems, including DC motors and three-phase asynchronous motors.

Simulation and experimental results show that the PID-NTSM controller achieves good tracking quality, fast response, high noise and uncertainty resistance, and significantly reduces chattering compared to traditional sliding mode controllers.

The direction of dissertation development

- Develop optimization and self-tuning mechanisms for PID-NTSM controllers to reduce reliance on manual tuning and improve adaptability to changing operating conditions.
- Combine the controller with disturbance or state observers to improve handling of large uncertainties, unmeasurable disturbances, and reduce the need for large control gain selection.
- Extend the application of the method to more complex systems such as multi-loop servo systems, robots, or other nonlinear mechatronic systems.
- Research the implementation of the algorithm on DSP platforms and low-cost microcontrollers, while further evaluating computational complexity, real-time latency, and integration capabilities in industrial control systems.

LIST OF THE PUBLICATIONS RELATED TO THE DISSERTATION

[CT.1] **Minh Trieu, N.**, Tan No, N., Nguyen Vu, T., & Thinh, N. T. (2025). Chattering-Free PID-Nested Nonsingular Terminal Sliding Mode Controller Design for Electrical Servo Drives. *Mathematics*, 13(7), 1197. (SCIE Q1)

[CT.2] **Minh Trieu N**, Tan No N, Nguyen Vu T, Truong Thinh N. Higher-Order PID-Nested Nonsingular Terminal Sliding Mode Control for Induction Motor Speed Servo Systems. *Actuators*. 2025; 14(12):580. <https://doi.org/10.3390/act14120580>. (SCIE Q2).

[CT.3] Trung Hieu NT, **Minh Trieu N**, Tri Dung D, Truong Thinh N. Advanced Sliding Mode Control Strategy for High-Performance 3D Concrete Printing. *Automation*. 2025; 6(2):22. (Scopus Q2)

[CT.4] **Nguyen Minh Trieu**, Do Truong Sang, Nguyen Truong Thinh. Robust Speed Control of DC Motors Using an Adaptive Fuzzy PID-Based Sliding Mode Approach. *Hội thảo Quốc gia lần thứ XXIX “Một số vấn đề chọn lọc của Công nghệ thông tin và Truyền thông”* (VNICT 2025).